PHYSICAL REVIEW B **72**, 064107 (2005)

# Enhancement of the piezoelectric response of tetragonal perovskite single crystals by uniaxial stress applied along the polar axis: A free-energy approach

Marko Budimir, Dragan Damjanovic,* and Nava Setter

*Ceramics Laboratory, Materials Institute, École polytechnique fédérale de Lausanne - EPFL, 1015, Lausanne, Switzerland*

(Received 18 April 2005; revised manuscript received 3 June 2005; published 10 August 2005)

The influence of the uniaxial bias stress on the piezoelectric properties of tetragonal $BaTiO_3$ and $PbTiO_3$ monodomain crystals is modeled in the framework of the phenomenological Landau-Ginzburg-Devonshire theory. It is shown that tensile and compressive stresses, both applied along the spontaneous polarization direction, reduce and enhance the piezoelectric response, respectively. The enhancement effect is due to the flattening of the free-energy profile and the corresponding dielectric softening of crystals, caused by the compressive stress. In $BaTiO_3$ crystals, at temperatures close to the tetragonal-orthorhombic phase transition temperature, the free-energy profile flattening and dielectric softening are the largest along axes perpendicular to the polarization direction, facilitating thus the polarization rotation away from the $[001]_c$ polar axis. The resulting enhancement of the shear piezoelectric coefficient is directly responsible for the increase of the longitudinal piezoelectric coefficient along the $[111]_c$ axis. At temperatures deep within the tetragonal phase in $BaTiO_3$, and over the whole ferroelectric region of $PbTiO_3$, the flattening of the free-energy profile and the dielectric softening by compressive stress are the strongest along the polar axis. The resulting enhancement of the longitudinal piezoelectric coefficient is thus the largest along the polar $[001]_c$ direction. These results, which can be applied to other perovskite crystals, have broad implications.

DOI: 10.1103/PhysRevB.72.064107 PACS number(s): 77.84.Dy, 77.65.Bn

## I. INTRODUCTION

The anisotropy of the piezoelectric effect in perovskite crystals and its enhancement along nonpolar axes have been a subject of intensive studies in the past several years.[1,2] In rhombohedral perovskite crystals the spontaneous polarization lies along the $[111]_c$ pseudocubic axis, while the largest longitudinal piezoelectric response is measured along the $[001]_c$ pseudocubic direction; in tetragonal crystals, with the spontaneous polarization parallel to the $[001]_c$ axis, the largest longitudinal piezoelectric response is observed close to the $[111]_c$ axis.[3,4] The effect is observed in many simple ($BaTiO_3$,[3] $KNbO_3$[5,6]) and complex perovskites [$Pb(Zr,Ti)O_3$,[7–10] $Pb(Mg_{1/2}Nb_{2/3})O_3$-$PbTiO_3$,[1] $BiScO_3$-$PbTiO_3$[11,12]] and both in crystals with so called “engineered domain structure”[13] and in monodomain single crystals.[14–16] Lead titanate, $PbTiO_3$, is an important exception to this behavior. It exhibits the largest longitudinal piezoelectric response along the polar axis over the whole temperature range where the ferroelectric tetragonal phase is stable; this behavior can be traced to the low ratio of the shear and longitudinal piezoelectric coefficients (or, which is equivalent, to the low dielectric anisotropy) in $PbTiO_3$.[4,17]

In materials with multiple ferroelectric-ferroelectric phase transitions, such as $BaTiO_3$, the intrinsic piezoelectric anisotropy discussed above is strongly temperature dependent and can be particularly large near the ferroelectric-ferroelectric phase transitions.[17–20] In complex solid solutions exhibiting a morphotropic phase boundary, such as $Pb(Zr,Ti)O_3$, the anisotropy depends on the composition, being the largest at the morphotropic phase boundary.[21,22] Large electric fields and uniaxial stresses applied along nonpolar directions also enhance the piezoelectric response away from the polar axis.[10,23–26] In all these cases the enhancement of the piezoelectric response along off-polar axis can be understood by considering the facilitated polarization rotation, i.e., the large dielectric susceptibility perpendicular to the polarization direction and consequently the large shear piezoelectric coefficient.[17]

It has been recently shown using Landau-Ginzburg-Devonshire phenomenological approach that a significant increase in the piezoelectric response of tetragonal $BaTiO_3$ monodomain single crystals may be expected when a strong electric field bias is applied antiparallel to the polarization.[27] An important difference is observed in the behavior of the tetragonal $BaTiO_3$ at low and high temperatures. At temperatures close to the tetragonal-orthorhombic phase transition temperature, the mechanism of the piezoelectric enhancement away from polar axes is the polarization rotation (an increase in the permittivity perpendicular to the polarization) and only a small enhancement is observed along the polar axis. At temperatures closer to the tetragonal-cubic phase transition temperature, the dominant enhancement of the piezoelectric response takes place along the polar axis and can be traced to the softening of the dielectric response along the polar direction by the electric field applied against the spontaneous polarization. At these temperatures, the polarization rotation that was invoked in many recent reports as the origin of the enhanced piezoelectric response in perovskite materials,[10,23] no longer plays the dominant role. $PbTiO_3$, which adopts only the tetragonal ferroelectric structure, behaves at all temperatures as $BaTiO_3$ in this high temperature region:[4] at electric bias fields applied antiparallel to the polarization, it exhibits the largest enhancement of the piezoelectric response along the polar axis[28] and the polarization rotation contributes relatively modestly to the response away from the polar direction.

Considering the above results, a following question can be posed: is there a deeper, common mechanism for the enhancement of piezoelectric properties away from and along the polar axis? In this paper, we attempt to answer this question by considering the piezoelectric response and its anisotropy in tetragonal $BaTiO_3$ and $PbTiO_3$ at uniaxial mechanical stresses applied along the polar axis. We show that the common denominator for the piezoelectric response enhancement away from and along the polar axis is the flattening of the Gibbs free energy profile of these crystal systems. The results obtained have broad implications and can be extended to explain the improved piezoelectric response in the vicinity of the morphotropic phase boundary of complex solid solutions, the enhancement of the piezoelectric response along and away from polar axis caused by electric field bias and the temperature driven enhancement of piezoelectric properties near ferroelectric-ferroelectric phase transitions.

## II. ELASTIC GIBBS FREE ENERGY

The influence of the hydrostatic and biaxial stress on dielectric properties of $BaTiO_3$ and $Pb(Zr,Ti)O_3$ has been discussed using the phenomenological Landau-Ginzburg-Devonshire theory in the past.[29–32] Experimental results on effect of stress on electro-mechanical properties have been recently reported for a number of complex relaxor ferroelectrics crystals with large piezoelectric anisotropy.[25,26,33,34] In this paper we investigate the effect of uniaxial stress applied along the polar $[001]_c$ direction on the dielectric and piezoelectric response of the tetragonal phase of $BaTiO_3$ and $PbTiO_3$ monodomain single crystals.

If one considers a 4mm tetragonal ferroelectric crystal with the zero external electric field and with a stress applied along the polar axis, the elastic Gibbs free energy $\Delta G$, expanded up to the sixth power of polarization, is given by[29,30,35–37]

$$\Delta G = \alpha_1 P_3^2 + \alpha_{11} P_3^4 + \alpha_{111} P_3^6 - \frac{1}{2} s_{11}^D X_3^2 - Q_{11} X_3 P_3^2, \quad (1)$$

where $X_3$ and $P_3$ are the applied mechanical bias stress and the polarization along the polar $[001]_c$ axis, respectively. If the stress is compressive, the value of $X_3$ is negative, by definition.[38] For barium titanate, the coefficients $\alpha$ and electrostrictive constants $Q$ are taken from Ref. 39, while the value of the elastic compliance $s_{11}^D$ at constant polarization is taken as $9 \times 10^{-12}\ \mathrm{m^2/N}$ at all temperatures within the tetragonal phase.[40] Coefficients for lead titanate are taken from Ref. 41 and $s_{11}^D = 8 \times 10^{-12}\ \mathrm{m^2/N}$.

As will be shown in Sec. III, a sufficiently high compressive stress $X_3$ can switch the polarization $P_3$ by 90°. The result of switching is so called an $a$-domain of the tetragonal phase, denoted here as $T_{90°}$ and characterized by $P_2 \neq 0$ or $P_1 \neq 0$ and $P_3 = 0$. In addition, barium titanate transforms into orthorhombic phase at $T = 278$ K by developing a polarization component along the $[010]_c$ axis, such that $P_2 = P_3 \neq 0$ and $P_1 = 0$. This phase is unstable in the temperature region of the tetragonal phase stability. To investigate the effect of the stress $X_3$ on the polarization switching by 90°, on the polarization rotation in the $(100)_c$ plane, and on the stability of the tetragonal phase of $BaTiO_3$, especially near the orthorhombic-tetragonal phase transition temperature, we shall consider in Sec. IV the following extended free energy function, assuming $P_2 \neq 0$:[29,30,35–37]

$$\begin{aligned}\Delta G = {} & \alpha_1 (P_3^2 + P_2^2) + \alpha_{11}(P_3^4 + P_2^4) + \alpha_{12} P_2^2 P_3^2 + \alpha_{111}(P_3^6 + P_2^6) \\ & + \alpha_{112}(P_2^4 P_3^2 + P_2^2 P_3^4) - \frac{1}{2} s_{11}^D X_3^2 - Q_{11} X_3 P_3^2 - Q_{12} X_3 P_2^2. \end{aligned} \quad (2)$$

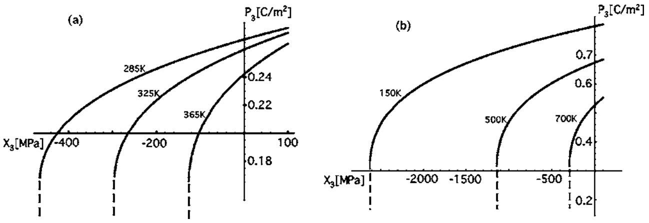

FIG. 1. The stress dependence of polarization in the $[001]_c$ direction of the tetragonal (a) $BaTiO_3$ and (b) $PbTiO_3$ at several temperatures. For each temperature there is a critical value of the compressive stress (negative values) that causes the polarization switching by 90°.

For the purposes of this paper we ignore (i) the rhombohedral phase ($P_1 = P_2 = P_3 \neq 0$) which in $BaTiO_3$ is stable below 183 K, (ii) the polarization rotation in the $(110)_c$ plane, as well as (iii) the switching of $P_3$ by 90° from $[001]_c$ to $[100]_c$ axis. Due to the symmetry of the tetragonal phase the latter is equivalent to the 90° switching from the $[001]_c$ to the $[010]_c$ axis, which is taken into account by Eq. (2).

## III. DEPENDENCE OF POLARIZATION, DIELECTRIC SUSCEPTIBILITY, AND PIEZOELECTRIC COEFFICIENTS ON UNIAXIAL STRESS

The stress dependences of spontaneous polarization, dielectric susceptibility, and piezoelectric coefficients for the tetragonal phase can be calculated from the condition for the elastic Gibbs free energy minimum,[37] $\partial G / \partial P_3 = 0$. The stress dependence of the spontaneous polarization, $P_3(X_3)$, is shown in Fig. 1 for $BaTiO_3$ and $PbTiO_3$ at selected temperatures. A tensile stress applied along the $[001]_c$ increases the tetragonality and the polarization of each material. For a compressive stress (i.e., $X_3 < 0$), the polarization $P_3$ decreases, and at some critical stress, which is a function of temperature, it drops to zero. This stress corresponds to the compressive stress necessary to switch the polarization by 90°, from $[001]_c$ to $[100]_c/[010]_c$ axis and is equivalent to the coercive electric field in the polarization-electric field hysteresis; see Ref. 27. We shall return to this case in the next section. In this section we discuss crystals properties only for stresses where $P_3 > 0$, and $P_2 = 0$.

The dielectric susceptibility $\eta_{ij}$ in the tetragonal phase ($\eta_{11} = \eta_{22}, \eta_{33}$) can be calculated[29,30,35–37] from Eq. (2) as $1/\varepsilon_0 \eta_{ij} = \partial^2 G / \partial P_i \partial P_j$, where $\varepsilon_0$ is the permittivity of vacuum. From Eq. (2) one obtains for the susceptibility perpendicular to the spontaneous polarization $\varepsilon_0 \eta_{11} = [2\Lambda_1$

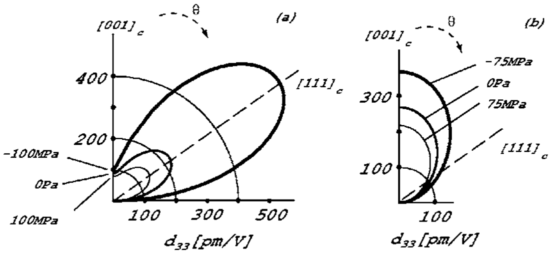

FIG. 2. The orientation dependence of the longitudinal piezoelectric coefficient, $d^*_{33}(\vartheta)$, in BaTiO$_3$ at (a) 285 K and (b) 365 K for different values of bias stress $X_3$. Note that from Eq. (4) $d^*_{33}(\vartheta)=d^*_{33}(-\vartheta)$.

$+2\alpha_{12}P_3^2(X_3)+2\alpha_{112}P_3^4(X_3)]^{-1}$, where $\Lambda_1=\alpha_1-Q_{12}X_3$, and for the susceptibility along the polar direction $\varepsilon_0\eta_{33}=[2\Lambda_3+12\alpha_{11}P_3^2(X_3)+30\alpha_{111}P_3^4(X_3)]^{-1}$, where $\Lambda_3=\alpha_1-Q_{11}X_3$. The shear, transverse and longitudinal piezoelectric coefficients in the crystallographic coordinate system are given, respectively, as[37]

$$d_{15}=\varepsilon_0\eta_{11}(X_3)Q_{44}P_3(X_3),$$

$$d_{31}=2\varepsilon_0\eta_{33}(X_3)Q_{12}P_3(X_3), \tag{3}$$

$$d_{33}=2\varepsilon_0\eta_{33}(X_3)Q_{11}P_3(X_3),$$

where $Q_{ij}$ are the electrostrictive constants. The orientation dependence of the longitudinal piezoelectric coefficient can be expressed as[17]

$$d^*_{33}(\vartheta)=d_{33}\cos^3\vartheta+(d_{31}+d_{15})\cos\vartheta\sin^2\vartheta, \tag{4}$$

where $\vartheta$ is the angle between the polar axis and the measuring filed [note: the measuring field (stress or electric field) is a weak field applied to measure the piezoelectric coefficient, not the bias field $X_3$]. Asterisk denotes the longitudinal coefficient in the rotated coordinate system, and $d_{im}$ stands for piezoelectric coefficients in the crystallographic coordinate system. The calculated orientation dependence of $d^*_{33}(\vartheta)$ is shown in Figs. 2 and 3 for selected uniaxial stresses applied to the tetragonal BaTiO$_3$ and PbTiO$_3$ along the polar $[001]_c$ axis. For BaTiO$_3$, the calculations have been done for $T=285$ K [Fig. 2(a)], close to the tetragonal-orthorhombic phase transition temperature ($T=278$ K) and $T=365$ K [Fig. 2(b)], closer to the tetragonal-cubic phase transition temperature (393 K). Calculations for PbTiO$_3$ have been done for $T=700$ K and $T=300$ K.

Barium titanate shows a qualitative change in the behavior as the temperature changes from $T=285$ K to $T=365$ K. At 285 K, the $d^*_{33}(\vartheta)$ in BaTiO$_3$ exhibits its maximum value along a direction ($\vartheta_{\max}\approx 50°$) that lies close to the $[111]_c$ axis. The value of $d^*_{33}(\vartheta_{\max})$ has a strong dependence on the applied stress. At $T=285$ K, for $X_3=0$, $d^*_{33}(\vartheta_{\max})=227$ pm/V. If one applies a tensile bias stress, the calculations predict that $d^*_{33}(\vartheta_{\max})$ will decrease. On the other hand, the compressive stress will enhance this piezoelectric coefficient. As shown in Fig. 2, at the compressive stress $X_3=-100$ MPa, $d^*_{33}(\vartheta_{\max})=654$ pm/V. This is a huge increase with respect to the zero stress value along the polar axis $[d^*_{33}(\vartheta=0°)=d_{33}=89$ pm/V$]$, as well as with respect to the maximum value $d^*_{33}(\vartheta_{\max})=227$ pm/V at $X_3=0$. It is clearly seen from Fig. 2(a) that both the enhancement effect by the compressive and reduction effect by the tensile stress are minimal along the polar axis and are the largest approximately along the $[111]_c$ axis.

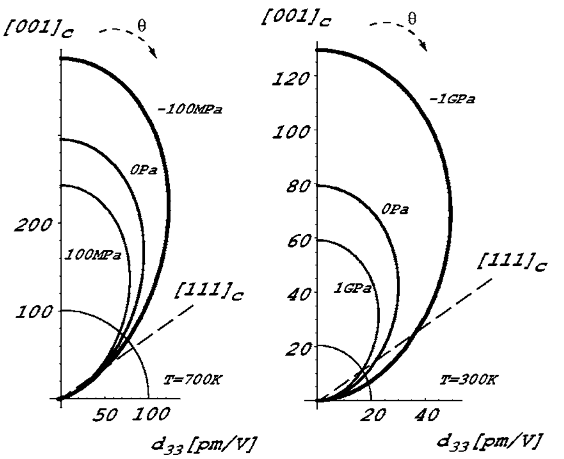

FIG. 3. The orientation dependence of the longitudinal piezoelectric coefficient, $d^*_{33}(\vartheta)$, in PbTiO$_3$ at 700 K and 300 K for different values of bias stress $X_3$. Note that from Eq. (4) $d^*_{33}(\vartheta)=d^*_{33}(-\vartheta)$.

Deeper in the tetragonal region of BaTiO$_3$, at $T=365$ K, one has again an enhancement of the piezoelectric response by the compressive stress and reduction by the tensile stress. However, the maximum response is now along the $[001]_c$ axis; see Fig. 2(b). At these temperatures the condition for having a maximum in $d^*_{33}(\vartheta)$ along a nonpolar direction is not fulfilled,[4] so the piezoelectric response exhibits the maximum value along the polar axis. Similarly to what is predicted for lower temperatures, the tensile stress decreases the piezoelectric coefficient $d^*_{33}(\vartheta)$, while the compressive stress enhances it. At $X_3=-75$ MPa and at 365 K, the maximum $d^*_{33}(\vartheta=0)$ is 469 pm/V, compared to 268 pm/V at $X_3=0$.

Qualitatively similar results can be shown for PbTiO$_3$; see Figs. 3(a) and 3(b). Analogous to the results for BaTiO$_3$ deep in the tetragonal phase, the maximum $d^*_{33}(\vartheta)$ and its maximum enhancement by the compressive stress in PbTiO$_3$ are observed along the polar axis. For example, at $T=700$ K, the compressive stress of $X_3=-100$ MPa will give approximately the 150% increase of $d^*_{33}(\vartheta)$ along the $[001]_c$ axis, while at $T=300$ K, the compressive stress of $X_3=-1000$ MPa increases $d^*_{33}(\vartheta_{\max}=0°)$ by over 160% (Fig. 3). In contrast to BaTiO$_3$, however, this behavior does not qualitatively change as PbTiO$_3$ is cooled toward $T=0$ K—this crystal stays strongly tetragonal and never exhibits a maximum of its longitudinal piezoelectric response along directions away from the polar axis.[42]

On the simple phenomenological level, one can understand above results by considering the stress dependences of dielectric susceptibilities $\eta_{ij}$ and piezoelectric coefficients $d_{im}$, depicted for the tetragonal BaTiO$_3$ in Fig. 4 and for PbTiO$_3$ in Fig. 5. The $d_{31}$ coefficient is sufficiently small under these conditions and can be neglected in the discus-

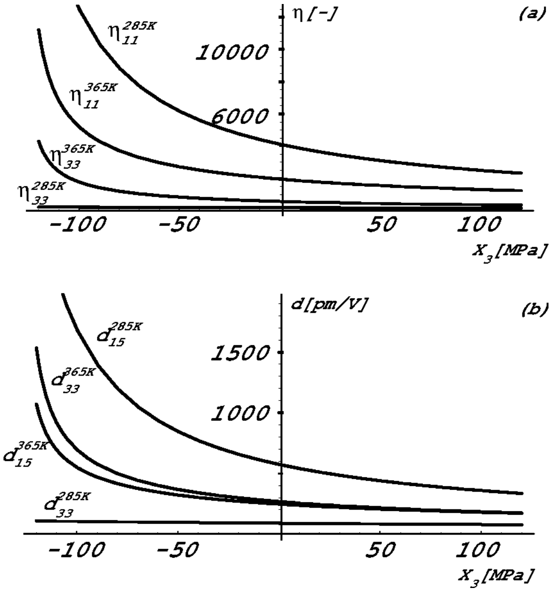

FIG. 4. (a) Susceptibilities, $\eta_{11}$ and $\eta_{33}$, and (b) piezoelectric coefficients, $d_{33}$ and $d_{15}$, of $BaTiO_3$ as a function of the bias mechanical stress $X_3$ at 285 K and 365 K.

sion; however, this coefficient was taken into account to calculate $d_{33}^{*}(\vartheta)$ shown in Figs. 2 and 3. For the tetragonal $BaTiO_3$, at $T=285$ K, close to the tetragonal-orthorhombic phase transition, the compressive bias stress increases $\eta_{11}$ while $\eta_{33}$ remains small, Fig. 4(a). The large $\eta_{11}$ implies an easier polarization rotation in $(100)_c$ or $(010)_c$ plane, away from the polar axis $[001]_c$, and leads therefore to a high $d_{15}$ coefficient [see Ref. 17, Eq. (4), and Fig. 4(b)]. Under conditions of a large dielectric anisotropy (large $\eta_{11}/\eta_{33}$ ratio), $d_{15}$ dominates Eqs. (5) and the maximum of $d_{33}^{*}(\vartheta)$ appears approximately along the $[111]_c$ axis.[4] It is important to note that the proximity of the tetragonal-orthorhombic phase transition temperature leads by itself to the maximum of $d_{33}^{*}(\vartheta)$ along the $[111]_c$ axis.[17] The effect is now considerably enhanced by the application of the compressive bias stress.

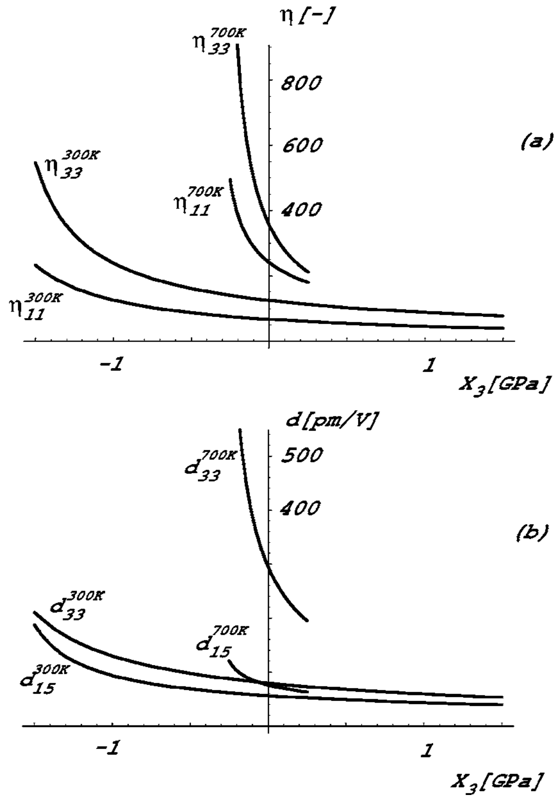

FIG. 5. (a) Susceptibilities, $\eta_{11}$ and $\eta_{33}$, and (b) piezoelectric coefficients, $d_{33}$ and $d_{15}$, of $PbTiO_3$ as a function of the bias mechanical stress $X_3$ at 300 K and 700 K.

At higher temperatures the dielectric anisotropy $\eta_{11}/\eta_{33}$ in $BaTiO_3$ is reduced; see Fig. 4(a). A smaller $\eta_{11}$ leads to a smaller $d_{15}$ [see Eq. (4) and Fig. 4] implying that the term containing $d_{33}$ now dominates Eq. (5). Therefore, the maximum in $d_{33}^{*}(\vartheta)$ appears along the polar axis;[4] see Fig. 3(b). By applying the compressive stress, the maximum $d_{33}^{*}(\vartheta=0°)$ increases; see Fig. 3(b). The enhancement of the maximum $d_{33}^{*}(\vartheta=0°)$ by compressive stress $X_3$ is now primarily due to the dielectric softening of the crystal *along* the polar axis. Thus, at this temperature range, the compressive stress-assisted polarization rotation no longer plays the dominant role in the enhancement of the longitudinal piezoelectric coefficient.

Figure 4(a) shows that, throughout the tetragonal phase of $BaTiO_3$, the compressive stress causes softening of the dielectric properties both parallel and perpendicular to the polar axis. The tensile stress has the opposite effect. The direction along which the stress-assisted dielectric softening is dominant, and the direction of the maximal piezoelectric response, are determined by the temperature of the system. One should note that tensile stress increases the tetragonality (polarization) while the compressive stress reduces it. Thus, despite the reduced polarization [see Eq. (4)], the compressive stress enhances the permittivity and consequently the piezoelectric coefficients. The enhancement of the material response by the compressive stress is due to the reduced stability of the polarization that is made more susceptible to a change by external fields. This point will be discussed further in the next section.

Exactly the same way of reasoning can be applied for the tetragonal $PbTiO_3$. The important difference is that, since there are no ferroelectric-ferroelectric phase transitions in this crystal, the maximum piezoelectric response lies always in the direction of the spontaneous polarization. In $PbTiO_3$, therefore, the stress causes the same effect as in the tetragonal $BaTiO_3$ at higher temperatures and the enhancement of the piezoelectric response is dominated by the dielectric softening along the polar axis. The enhancement effect along the polar axis in $PbTiO_3$ is particularly pronounced at higher temperatures where $\eta_{33} > \eta_{11}$.[17]

As already mentioned in the Introduction, the qualitatively similar behavior was reported[27] in $BaTiO_3$ when an electric bias field was applied along or antiparellel to the polar direction. This similar response of perovskite crystals to a variation of different parameters suggests a common underlying mechanism for the origins of the piezoelectric anisotropy and its enhancement, no matter what the considered variable is—the temperature, the electric field, the mechanical stress, or the composition.

## IV. FLATTENING OF THE ELASTIC GIBBS FREE-ENERGY PROFILE BY COMPRESSIVE STRESS

In this section we discuss the Gibbs free energy for the tetragonal $BaTiO_3$ at $T=285$ K and $PbTiO_3$ at $T=300$ K, as a function of the uniaxial mechanical stress bias, $X_3$, applied along the polar axis. It will be shown that the dielectric softening of the crystal perpendicular to and along the polar axis, and the resulting enhancement of the piezoelectric response, are a consequence of the stress-assisted flattening of the Gibbs free-energy profile.

In the ferroelectric $BaTiO_3$ and $PbTiO_3$, the spontaneous polarization is related to a temperature induced atoms displacement with respect to their ideal positions in the cubic paraelectric phase.[43] External bias and measuring fields shift atoms and modify the polarization. The elastic Gibbs free energy in Eq. (2) thus reflects the free energy of the crystal as a function of atoms shifts by external fields or temperature variation. A flatter profile of $\Delta G(P_2,P_3)$ is a manifestation of the higher susceptibility of the system to atoms displacement, and signifies therefore enhanced dielectric susceptibility and piezoelectric coefficients. In the previous section we have shown that the enhancement of the dielectric and piezoelectric properties of the crystals by external stress is strongly anisotropic. In this section we demonstrate that the softening of the material response is a direct consequence of the anisotropic flattening of the Gibbs free energy profile by the external stress.

To support the following discussion, we first show in Fig. 6 a three-dimensional plot of $\Delta G(P_2,P_3)$ for $BaTiO_3$ ($T=285$ K,$X_3=-100$ MPa) and for $PbTiO_3$ ($T=300$ K,$X_3=-1000$ MPa). The thick solid lines represent $\Delta G(P_2)$ at the equilibrium spontaneous polarization $P_3$ for a given compressive stress $X_3$ ($P_3=0.257$ C/m$^2$ in $BaTiO_3$ and 0.654 C/m$^2$ in $PbTiO_3$). The $\Delta G(P_2)$ profile reflects a polarization rotation away from the polar axis and in the $(100)_c$ plane, caused by a weak measuring field applied along the $[010]_c$ axis. The dashed lines represent $\Delta G(P_3)$ for $P_2=0$ and correspond to measurements along the polar axis. Black dots mark approximate positions of the stable and metastable tetragonal, orthorhombic and cubic phases. $T_{0°}$ indicates the tetragonal phase with the polarization along the $[001]_c$ axis ($P_3\neq 0,P_2=0$), and $T_{90°}$ the tetragonal phase with the polarization switched by 90°, i.e., along the $[010]_c$ axis ($P_3=0,P_2\neq 0$). The cross sections of $\Delta G(P_2,P_3)$ are shown in Fig. 7 for $BaTiO_3$ ($T=285$ K, for $X_3=-100$, 0, +100 MPa) and in Fig. 8 for $PbTiO_3$ ($T=300$ K, for $X_3=-1000$, 0, +1000 MPa). Note that, while Fig. 6 is calculated for compressive stress only, Figs. 7 and 8 include also data for stress free crystals and crystals under tensile stress $X_3$.

We first discuss the results for $BaTiO_3$ at $T=285$ K shown in Fig. 7. The $\Delta G(P_2=0,P_3)$ given in Fig. 7(a) reflects the susceptibility of the crystal to dilatation and contraction of the polarization along the polar $[001]_c$ axis. Comparison of curves for the tensile (dashed-dotted line) and compressive stress (solid line) shows that, as the tetragonality decreases by the compressive stress, the $\Delta G(P_2,P_3)$ profile becomes somewhat flatter indicating an improved movement of atoms along the $[001]_c$ axis. However, the effect is modest, as it is shown in a small increase in the permittivity and the piezoelectric coefficient along the polar axis, Fig. 4. The effect is strikingly stronger for $\Delta G(P_2;P_3=0.257)$, Fig. 7(b), which reflects a change in the $\Delta G$ when the external measuring field has a component perpendicular to the polar axis $[001]_c$. For the dielectric response this situation corresponds to the polarization rotation in the $(100)_c$ plane, away from the $[001]_c$ and toward the $[010]_c$ axis; for the piezoelectric response the situation corresponds to the shear effect. The compressive stress $X_3$ strongly flattens the $\Delta G(P_2;P_3=0.257)$ profile, Fig. 7(b), leading to a considerable increase in $\eta_{11}$ and $d_{15}$; see Fig. 4. The flattening of the $\Delta G$ profile along the polar axis (corresponding to the polarization dilatation and contraction) and within $(100)_c$ plane (corresponding to the polarization rotation) are compared in Fig. 7(c). The flattening of the $\Delta G$ profile is clearly anisotropic: the

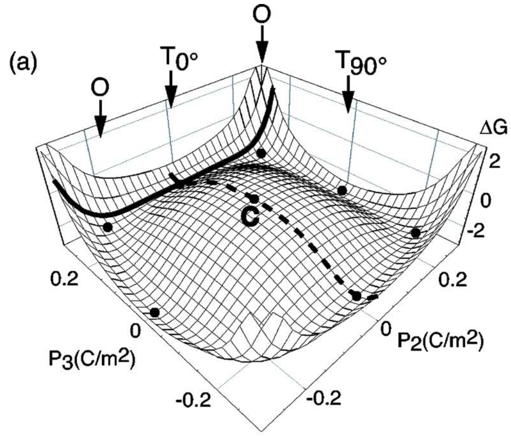

$BaTiO_3$, 285 K, $X_3$= -100 MPa

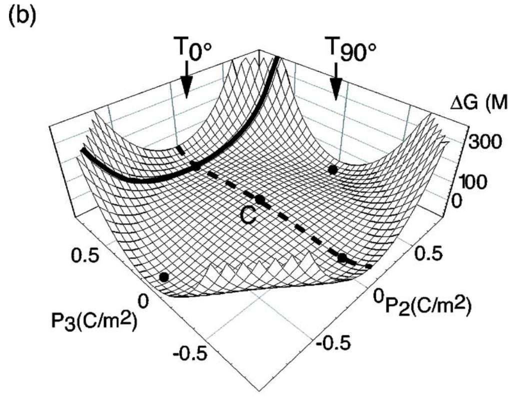

$PbTiO_3$, 300 K, $X_3$= -1 GPa

FIG. 6. (Color online) The Gibbs free energy [Eq. (2)] at compressive stress for (a) $BaTiO_3$ ($T=285$ K,$X_3=-100$ MPa) and (b) for $PbTiO_3$ ($T=300$ K,$X_3=-1000$ MPa). The thick solid lines represent $\Delta G(P_2)$ at equilibrium $P_3$ ($P_3=0.257$ C/m$^2$ in $BaTiO_3$ and 0.654 C/m$^2$ in $PbTiO_3$), reflecting the polarization rotation away from the polar axis in $(100)_c$ plane. The dashed lines represent $\Delta G(P_3)$ for $P_2=0$. Black dots mark approximate positions of the stable and metastable tetragonal, orthorhombic, and cubic phases. $T_{0°}$ indicates the tetragonal phase with polarization along the $[001]_c$ axis ($P_3\neq 0,P_2=0$), and $T_{90°}$ the tetragonal phase with polarization switched by 90°, i.e., along the $[010]_c$ axis ($P_3=0,P_2\neq 0$).

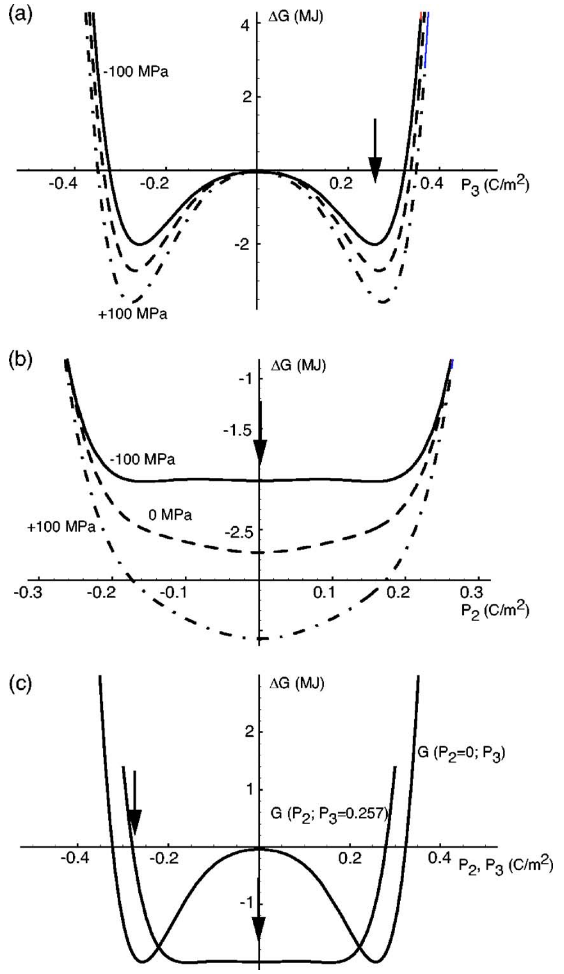

FIG. 7. (Color online) The profile of the Gibbs free energy at compressive (−100 MPa, solid lines), zero (dashed line), and tensile (+100 MPa, dashed-dotted line) stress for $BaTiO_3$ at $T=285$ K. (a) $\Delta G(P_3)$ for $P_2=0$, (b) $\Delta G(P_2)$ at equilibrium $P_3(P_3=0.257\ \mathrm{C/m^2})$, and (c) comparison of the flatness of $\Delta G(P_2;P_3=0.257)$ and of $\Delta G(P_2=0;P_3)$. The former indicates the rotation of $P_3$ from the $[001]_c$ toward the $[010]_c$ axis in the $(100)_c$ plane, and the latter indicates a dilatation or a reduction of the polarization along the $[001]_c$ axis. The arrows show a general position of the equilibrium tetragonal state. Compare with Fig. 6.

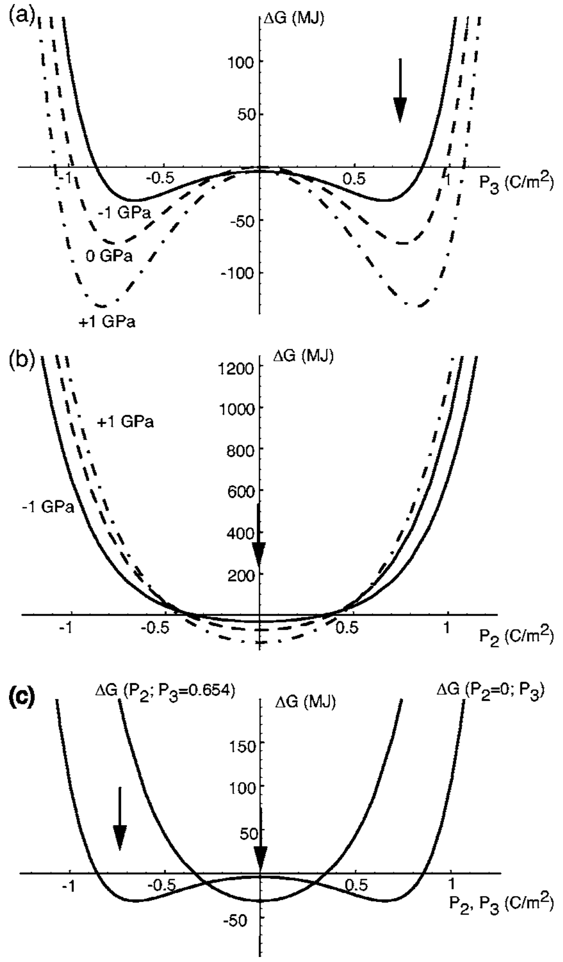

FIG. 8. The profile of the Gibbs free energy at compressive (−1000 MPa, solid lines), zero (dashed line), and tensile (+1000 MPa, dashed-dotted line) stress for $PbTiO_3$ at $T=300$ K. (a) $\Delta G(P_3)$ for $P_2=0$. (b) $\Delta G(P_2)$ at equilibrium $P_3$ ($P_3=0.654\ \mathrm{C/m^2}$), and (c) the comparison of the flatness of $\Delta G(P_2;P_3=0.654)$ and of $\Delta G(P_2=0;P_3)$. The former indicates rotation of $P_3$ from the $[001]_c$ toward the $[010]_c$ axis in the $(100)_c$ plane and the latter indicates a dilatation or a reduction of the polarization along the $[001]_c$ axis. The arrows show a general position of the equilibrium tetragonal state. Compare with Fig. 6.

effect of the flattening on the polarization rotation (and on $\eta_{11}$ and $d_{15}$) is much stronger than on the polarization contraction (and on $\eta_{33}$ and $d_{33}$). This ultimately leads to a much larger enhancement of $d_{33}^*$ away from than along the polar axis, as shown in Fig. 2(a).

Similar to its effect on the free energy of $BaTiO_3$, the compressive stress has tendency to flatten the $\Delta G(P_2,P_3)$ polarization dependence in $PbTiO_3$, Figs. 8(a) and 8(b), and thus to enhance its piezoelectric response. However, the anisotropy of the $\Delta G(P_2,P_3)$ profile flattening in $PbTiO_3$ is at all temperatures qualitatively different from that in $BaTiO_3$ at 285 K. In $PbTiO_3$, the flattening is more pronounced along the polar axis, Fig. 8(c), than along the $[010]_c$ axis. Consequently, the contraction of the polarization along the $[001]_c$ axis is now at least as much important as the rotation in the $(010)_c$ plane. Using the same line of arguing as above, one sees that the longitudinal piezoelectric effect $d_{33}$ and susceptibility $\eta_{33}$ now increase more by the compressive stress, Fig. 5, than $d_{15}$ and $\eta_{11}$. The shear effect no longer dominates in Eq. (5) and the maximum $d_{33}^*$ and its maximum enhancement by the compressive stress appear along the polar axis.

At 365 K $BaTiO_3$ behaves similarly to $PbTiO_3$, and will not be discussed in detail. The polarization rotation effects in this temperature range are stronger in $BaTiO_3$ than in highly tetragonal $PbTiO_3$, but still do not dominate the piezoelectric response. Therefore, the maximum $d_{33}^*$ and its maximum enhancement appear along the polar axis; see Fig. 2(b). This is true for the tetragonal phase of $BaTiO_3$ above a certain critical temperature.[4]

We next discuss the stability of the polarization along $[001]_c$ axis when a compressive stress is applied on the crystal. A compressive stress leads to reduction of the polariza-

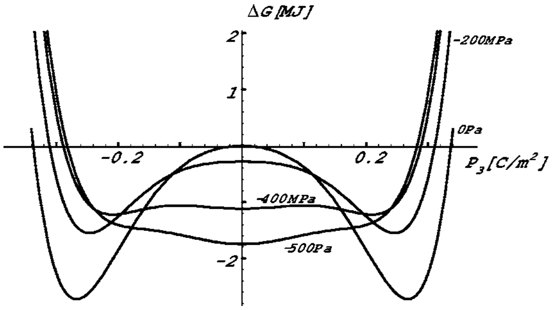

FIG. 9. The Gibbs free energy of the tetragonal $BaTiO_3$ at $T = 285$ K as a function of the applied compressive stress. At coercive stress the free energy develops a minimum for $P_3 = 0$ corresponding to a saddle point in the two-dimensional graph, indicating the 90° switching into the $(P_2 \neq 0; P_3 = 0)$ state. Compare with Figs. 1 and 6.

tion, which becomes zero at a certain coercive stress; see Fig. 1. In terms of the Gibbs energy, the $\Delta G(P_3)$ develops for sufficiently high compressive stress a minimum at $P_3 = 0$; see Fig. 9. As mentioned in Sec. II, this minimum does not correspond to the cubic phase, but to the switching by 90° into the tetragonal state characterized by $P_2 \neq 0$; $P_3 = 0$, indicated in Fig. 6 as $T_{90^\circ}$. That this state is not cubic but tetragonal, can be verified by analyzing the $\Delta G(P_2, P_3)$. The analysis shows that the minimum in $\Delta G(P_3)$, seen in Fig. 9 at, for example, 500 MPa, corresponds to a saddle point in the two dimensional $\Delta G(P_2, P_3)$ plot; the system does not stay in the cubic state but moves into $T_{90^\circ}$ state.

In systems with the first order phase transitions, such as $BaTiO_3$ and $PbTiO_3$, the phase transitions are hysteretic: the system can remain in a metastable state as long as this state represents a local minimum in $\Delta G$. Thus, switching from the tetragonal $T_{0^\circ}$ state $(P_2 = 0; P_3 \neq 0)$ to the tetragonal $T_{90^\circ}(P_2 \neq 0; P_3 = 0)$ state happens not when the minimum for $T_{90^\circ}$ becomes an absolute minimum, but when the minimum for $T_{0^\circ}$ transforms into an inflection point. In $BaTiO_3$, at 285 K, this happens at $X_3 < -400$ MPa, while the calculations in Sec. III were made for $X_3 = -100$ MPa. For all calculations, care was taken not to pass over the coercivity limit. Furthermore, an orthorhombic phase $(P_2 = P_3 \neq 0)$ appears in $BaTiO_3$ at 278 K. The stress applied along the $[001]_c$ can shift the tetragonal system into the $T_{90^\circ}$ state, while only temperature can develop the orthorhombic state. Thus, in Fig. 7(b), the curve for $X_3 = -100$ MPa has three minima: two for an incipient orthorhombic state (for $P_2$ between $-0.2$ and $-0.1$ $C/m^2$ and between $+0.1$ and $+0.2$ $C/m^2$) and one for $T_{0^\circ}$ state for $P_2 = 0$. Even though $T_{0^\circ}$ is not an absolute minimum, the system will stay in that state as long as it is a local minimum. Only when the temperature is sufficiently decreased and this minimum becomes an inflection point, the system will transform into the orthorhombic state.

We finally point out that results presented refer to thermodynamically ideal systems. Real crystals will have lower coercive fields and the described effects will be weaker. However, our calculations demonstrate general trends that can be expected from tetragonal perovskite crystals under the influence of the uniaxial stress applied along the polar axis.

## V. CONCLUSIONS

It is shown that the enhancement of the longitudinal piezoelectric response in $BaTiO_3$ and $PbTiO_3$ crystals by the compressive stress applied along the polar axis can be interpreted in terms of the profile flattening of the Gibbs free energy. This is true for the enhancement along the $[111]_c$ axis (in $BaTiO_3$ at 285 K) as well as along the $[001]_c$ axis in $PbTiO_3$ (throughout the tetragonal phase) and in $BaTiO_3$, at sufficiently high temperatures. The Gibbs free energy profile flattening by the compressive stress can be directly related either to the facilitated polarization rotation in $(100)_c$ plane or to the polarization contraction along the polar axis. The most important result is that both the polarization rotation (piezoelectric enhancement along nonpolar axes) and polarization contraction (piezoelectric enhancement along the polar axis) effects can be described by the common mechanism, i.e., the instability (the profile flattening) of the elastic Gibbs free energy.

We propose that the same approach can be applied to other perovskites to investigate origins of the piezoelectric effect enhancement (i) as a function of the composition in the vicinity of the morphotropic phase boundary, (i) as a function of the electric field bias, and (iii) as a function of temperature. The first steps in extending this method to temperature driven effects[21] suggests that the approach is indeed generally valid and that results presented in this paper thus have broad implications.

## ACKNOWLEDGMENTS

The authors acknowledge financial support of the Swiss National Science Foundation.

---

*Corresponding author. Email address: dragan.damjanovic@epfl.ch

[1] S. E. Park and T. R. Shrout, J. Appl. Phys. **82**, 1804 (1997).
[2] J. Kuwata, K. Uchino, and S. Nomura, Jpn. J. Appl. Phys., Part 1 **21**, 1298 (1982).
[3] S. Wada, S. Suzuki, T. Noma, T. Suzuki, M. Osada, M. Kakihana, S. E. Park, L. E. Cross, and T. R. Shrout, Jpn. J. Appl. Phys., Part 1 **38**, 5505 (1999).
[4] D. Damjanovic, F. Brem, and N. Setter, Appl. Phys. Lett. **80**, 652 (2002).
[5] K. Nakamura and Y. Kawamura, IEEE Trans. Ultrason. Ferroelectr. Freq. Control **47**, 750 (2000).
[6] K. Nakamura, T. Tokiwa, and Y. Kawamura, J. Appl. Phys. **91**, 9272 (2002).
[7] X. Du, U. Belegundu, and K. Uchino, Jpn. J. Appl. Phys., Part 1 **36**, 5580 (1997).
[8] X.-H. Du, J. Zheng, U. Belegundu, and K. Uchino, Appl. Phys.

Lett. **72**, 2421 (1998).

[9] D. V. Taylor and D. Damjanovic, Appl. Phys. Lett. **76**, 1615 (2000).

[10] R. Guo, L. E. Cross, S. E. Park, B. Noheda, D. E. Cox, and G. Shirane, Phys. Rev. Lett. **84**, 5423 (2000).

[11] S. Zhang, C. A. Randall, and T. R. Shrout, Appl. Phys. Lett. **83**, 3150 (2003).

[12] S. Zhang, C. A. Randall, and T. R. Shrout, J. Appl. Phys. **95**, 4291 (2004).

[13] S. Wada, H. Kakemoto, and T. Tsurumi, Mater. Trans., JIM **45**, 178 (2004).

[14] R. Zhang and W. Cao, Appl. Phys. Lett. **85**, 6380 (2004).

[15] R. Zhang, B. Jiang, and W. Cao, Appl. Phys. Lett. **82**, 3737 (2003).

[16] D. Damjanovic, M. Budimir, M. Davis, and N. Setter, Appl. Phys. Lett. **83**, 527 (2003).

[17] M. Budimir, D. Damjanovic, and N. Setter, J. Appl. Phys. **94**, 6753 (2003).

[18] D. Viehland, J. F. Li, and A. Amin, J. Appl. Phys. **92**, 3985 (2002).

[19] S. E. Park, S. Wada, L. E. Cross, and T. R. Shrout, J. Appl. Phys. **86**, 2746 (1999).

[20] Z. Yu, R. Guo, and A. S. Bhalla, Appl. Phys. Lett. **77**, 1535 (2000).

[21] D. Damjanovic, M. Budimir, M. Davis, and N. Setter, J. Mater. Sci. (to be published).

[22] M. Iwata, H. Orihara, and Y. Ishibashi, Ferroelectrics **266**, 57 (2002).

[23] H. Fu and R. E. Cohen, Nature (London) **403**, 281 (2000).

[24] L. Bellaiche, A. Garcia, and D. Vanderbilt, Phys. Rev. B **64**, 060103(R) (2001).

[25] D. Viehland and J. Powers, J. Appl. Phys. **89**, 1820 (2001).

[26] D. Viehland, L. Ewart, J. Powers, and J. F. Li, J. Appl. Phys. **90**, 2479 (2001).

[27] M. Budimir, D. Damjanovic, and N. Setter, Appl. Phys. Lett. **85**, 2890 (2004).

[28] Unpublished results.

[29] A. K. Goswami and L. E. Cross, Phys. Rev. **171**, 549 (1968).

[30] A. K. Goswami, J. Phys. Soc. Jpn. **21**, 1037 (1966).

[31] A. Amin, R. E. Newnham, and L. E. Cross, Phys. Rev. B **34**, 1595 (1986).

[32] V. G. Koukhar, N. A. Pertsev, and R. Waser, Phys. Rev. B **64**, 214103 (2001).

[33] E. A. McLaughlin, T. Q. Liu, and C. S. Lynch, Acta Mater. **52**, 3849 (2004).

[34] M. Davis, D. Damjanovic, and N. Setter, J. Appl. Phys. **95**, 5679 (2004).

[35] A. F. Devonshire, Philos. Mag. **42**, 1065 (1951).

[36] A. F. Devonshire, Philos. Mag. **40**, 1040 (1949).

[37] M. J. Haun, E. Furman, S. J. Jang, and L. E. Cross, Ferroelectrics **99**, 13 (1989).

[38] A. Amin, L. E. Cross, and R. E. Newnham, Ferroelectrics **99**, 145 (1989).

[39] A. J. Bell and L. E. Cross, Ferroelectrics **59**, 197 (1984).

[40] A. Schaefer, H. Schmitt, and A. Dörr, Ferroelectrics **69**, 253 (1986).

[41] M. J. Haun, E. Furman, S. J. Jang, H. A. McKinstry, and L. E. Cross, J. Appl. Phys. **62**, 3331 (1987).

[42] In the framework of the LGD theory, we assume that $PbTiO_3$ is 4mm tetragonal ferroelectric from 763 K to zero K; see M. J. Haun, E. Furman, S. J. Jang, H. A. McKinstry, and L. E. Cross, J. Appl. Phys. **62**, 3331 (1987); J. Kobayashi, Y. Uesu, and Y. Sakemi, Phys. Rev. B **28**, 3866 (1983); have reported a transition to an orthorhombic phase below 100 K; however, this result, to the best of our knowledge, has not been confirmed elsewhere. See also H. Mestric, R. A. Eichel, T. Kloss, K. P. Dinse, S. Laubach, S. Laubach, P. C. Schmidt, K. A. Schonau, M. Knapp, and H. Ehrenberg, Phys. Rev. B **71**, 134109 (2005).

[43] M. E. Lines and A. M. Glass, *Principles and Applications of Ferroelectrics and Related Materials* (Clarendon, Oxford, 1979).